Journal of Power Sources 195 (2010) 5167–5175

Contents lists available at ScienceDirect

Journal of Power Sources

journal homepage: www.elsevier.com/locate/jpowsour

Influence of carbon support microstructure on the polarization behavior of a polymer electrolyte membrane fuel cell membrane electrode assemblies

Abhishek Guha [a], Thomas A. Zawodzinski Jr. [b], David A. Schiraldi [a,*]

[a] Department of Macromolecular Science and Engineering and Case Advanced Power Institute, Case Western Reserve University, 10900 Euclid Avenue, 2100 Adelbert Rd, Cleveland, OH 44106-7202, United States
[b] Department of Chemical Engineering and Case Advanced Power Institute, Case Western Reserve University, 10900 Euclid Avenue, Cleveland, OH 44106, United States

ARTICLE INFO

Article history:
Received 20 January 2010
Received in revised form 1 March 2010
Accepted 2 March 2010
Available online 15 March 2010

Keywords:
Carbon nanofibers
Vulcan XC-72 carbon
Catalyst support
Support morphology
Membrane electrode assembly

ABSTRACT

The influence of carbon support morphology on the polarization behavior of a PEM fuel cell membrane electrode assembly has been investigated in this communication. Nanometer sized platinum electrocatalyst particles were deposited on lower surface area fibrous (carbon nanofibers) and particulate carbon supports (carbon blacks) by the well-documented ethylene glycol route for supported electrocatalyst synthesis. These supported catalyst systems were subsequently utilized to prepare catalyst inks and membrane electrode assemblies (MEA) in conjunction with a perflurosulfonated ionomeric membrane-Nafion®. Level of liquid Nafion binder in the supported catalyst inks was varied and the ramifications of such a variation on polarization behavior of the MEA determined. The trend in polarization performance was found to be independent of the carbon support morphology in the various ink compositions. The two varieties of carbon supports were also mixed together in various weight ratios and platinum was deposited by the glycol method. Key parameters such as the platinum content on carbon and platinum particle size were determined to be independent of the nature of the supports on which the particles had been deposited. The results indicate that lower surface area carbon supports of vastly contrasting morphologies can be interchangeably employed as catalyst support materials in a PEM fuel cell MEA.

1. Introduction

A membrane electrode assembly (MEA) is the heart of a polymer electrolyte membrane (PEM) fuel cell. Voltage–current characteristics or 'polarization' behavior of the MEA is strongly dependent, amongst other factors, on behavior of the supported catalyst layer within the MEA. This layer consists of nanosized precious metal electrocatalyst particles (such as platinum) deposited on a suitable support material, which is typically carbon. Carbon supports are available in varying morphologies and dimensions. The electrode layer in a PEM fuel cell MEA comprises of the catalyst particle, carbon support and an ionomer layer co-deposited to form a heterogeneous phase mixed conductor. Both the ionic as well as electronic transport characteristics of the electrode layer are crucial to the overall MEA performance.

Many diagnostic studies of PEM fuel cell polarization performances have been reported in the literature over the past few years. A substantial portion of the published work has focused on the ionomeric membrane in the MEA. In comparison, the volume of published literature devoted to detailed investigation of the supported catalyst layer is small. Part of the reason behind such a disparity is the practical difficulty in deconstructing the MEA and isolating the electrode layer post-fabrication and testing. Also precious few techniques for detailed study of such 'buried interfaces' are available.

Nevertheless, a few research groups have attempted to investigate key electrode properties such as electronic resistivity/conductivity of the electrode layer as well as influence of electrode layer topography on MEA performance. Giorgi et al. prepared PEM fuel cell cathodes with different concentrations of poly-(tetrafluoroethylene) or PTFE binder in the gas diffusion layer [1]. They found that PTFE content in the electrode layer influenced its porosity, which in turn had a bearing on the electrochemically active surface area of the electrode. An intermediate loading of PTFE was optimized in order to obtain sufficient hydrophobicity in the electrode layer while simultaneously extracting optimum performance out of the electrode layer.

A similar approach was adapted by Lee et al. who employed recast Nafion® as the catalyst binder in their electrode layers and investigated influence of the relative proportions of electrode com-

* Corresponding author. Tel.: +1 216 368 4172; fax: +1 216 368 4202.
E-mail addresses: david.schiraldi@case.edu, das44@case.edu (D.A. Schiraldi).

0378-7753/$ – see front matter © 2010 Elsevier B.V. All rights reserved.
doi:10.1016/j.jpowsour.2010.03.006

ponents on MEA performance [2]. The authors pointed towards ionic and diffusion resistances as the primary contributors to the linear potential drops in the ohmic region of the polarization curves. Xie et al. examined the surface and cross-section of the supported catalyst layer in the MEA using a variety of surface analysis techniques and correlated MEA performance to its structure and materials employed in the preparation [3]. Employing scanning electron microscopy (SEM) to examine MEA surfaces fabricated by the 'decal-method' [4,5], Xie and co-workers found that an ionomer rich 'skin' was present on the catalyst layer surface. A thicker skin led to higher oxygen diffusion resistance through to the catalyst particle sites as well as slower removal of water from the active sites. However, any potential influence of the skin on the electronic resistance of the electrode layer and the contact resistance between the electrode surface and the Nafion membrane was not studied.

Saab et al. at Los Alamos National Laboratories discussed a technique to measure the electronic resistance of a thin layer of carbon/Pt/Nafion fuel cell electrode composite material by a DC polarization route and then couple the information with ionic resistance measurements from AC impedance (ACI) analysis to compute overall resistance of the composite electrode layer [6]. A study by Stanic measured total ohmic resistances of various MEA electrode layers and correlated the data to microstructure of the electrode surface [7]. Wang et al. presented a novel route to examine microstructural features of direct methanol fuel cell (DMFC) electrodes by SEM [8]. Specialized analytical techniques such as proton induced X-ray emission (PIXE) and scanning electrochemical microscopy (SECM) were employed to observe electrode surface topography and distribution of active elements in the catalyst layer. A slew of recent publications have attempted to study the physico-chemical and electronic interactions at the catalyst–carbon support interface and the enhancement of catalytic activity through improved catalyst–support interaction [9,10]. These papers have investigated supported catalyst systems wherein the carbon support morphology ranges from spherical such as Vulcan XC-72 [11,12]; monolithic porous structures such as carbon aerogels [13] and novel fibrous supports such as carbon nanofibers [14].

In our work, influence of carbon support microstructure on the MEA fuel cell performance has been probed. Our previous research has shown that for PEM MEAs with supported catalyst layers synthesized using conventional processing techniques, lower surface area catalyst supports such as carbon nanofibers and Vulcan® XC-72 carbon black outperform higher surface area carbons such as activated carbon in fuel cell performance [15]. The contrasting morphologies of these carbon supports open the window to probing the 'topological' influence of carbon supports on catalyst layer performance. One of our primary objectives is to evaluate the polarization behavior of MEAs fabricated using catalyst inks with different carbon morphologies and increasing concentrations of the liquid Nafion binder.

Two families of lower surface area carbons have been mixed together in various weight ratios and platinum deposited on each carbon support mixture using the well-understood ethylene glycol route for electrocatalyst deposition [16–18]. The logic behind mixing the supports is that the expected benefits of a fibrous carbon support in the mixture (which can potentially provide a long continuous electronic conduction pathway) could be supplemented by providing improved fiber-to-fiber contact using the particulate carbon. For the platinum deposited on the various support mixtures, key parameters such as the platinum content (weight%), average particle size and relative availability of the platinum surface area for catalytic activity, have been compared and contrasted for the various support mixtures.

2. Experimental

2.1. Platinum catalyst deposition on carbon supports and their mixtures

Graphitic carbon nanofibers or CNF (Pyrograf®-III; PR-19-HHT grade) were obtained from Applied Sciences Inc., Cedarville, OH. The HHT notation indicates that the carbon fibers had been heat-treated to temperatures up to 3000 °C [19]. These nanofibers are a highly electronically conductive form of carbon typically 100–150 nm in diameter. The iron catalyst content in the supplied nanofibers is less than 100 ppm [19]. Amorphous carbon black (Vulcan® XC-72 carbon) was supplied by Cabot Corporation, Billerica, MA. Vulcan XC-72 is a conductive carbon black with low sulfur content. It is a very popular electrocatalyst support widely used in PEM and DMFC systems.

Structurally, the nanofibers exist as coaxial graphene cylinders with hollow cores whereas the Vulcan XC-72 carbon is spherical in nature. Carbon support mixtures were prepared by physically combining together the CNF and Vulcan XC-72 carbons. Three such mixtures were prepared where the relative weight concentration (w/w%) of CNF/Vulcan XC-72 were (25/75), (50/50) and (75/25), respectively. Prior to mixing, the carbon nanofibers had been acid-modified or chemically 'functionalized'. Functionalization is necessitated by the chemically inert nature of the graphitic CNF, which make catalyst deposition extremely difficult otherwise. Further details about the functionalization procedure are discussed in our prior publication [20]. No such modification was carried out on the Vulcan XC-72 carbon black because of its comparatively higher reactive surface area due to a disordered microstructure.

Surface area measurements of the two control carbon supports (100% by weight functionalized CNF and 100% Vulcan XC-72) as well as the various support mixtures was carried out by Micromeritics Analytical Services, Norcross, GA. Adsorption isotherms were determined by nitrogen adsorption over the carbon samples at 77 K. BET surface areas (in $m^2\,g^{-1}$) of the sample were calculated by applying the BET equation to the adsorption isotherms.

Platinum was deposited on the control carbons and their mixtures by following for most part, an optimized 'polyol' reduction of hydrogen hexachloroplatinate or chloroplatinic acid ($H_2PtCl_6{\cdot}6H_2O$, Aldrich) using ethylene glycol [20]. The chloroplatinic acid was chemically reduced to colloidal platinum which then adsorbed onto the functionalized carbon support surface. The flask was allowed to cool and the supported catalyst filtered and washed with a liter of deionized water and allowed to dry for 24 h. Normally, after the supported catalyst has dried, it is subjected to an 'activation' procedure which converts the platinum colloid (platinum in its oxide form) to elemental platinum. The activation or 'heat-treatment' procedure has been shown to have a strong bearing on catalyst properties such as, particle size, morphology, dispersion of the metal on the support, alloying degree, active site formation, catalytic activity and stability [21]. The activation procedure also ensures that the platinum particles stay adhered to the functional groups created on the carbon support surface as a result of the functionalization process. The end objective is to ensure that the bulk average particle sizes of the catalyst particles is in the 2–5 nm range for acceptable electrocatalytic activity, especially towards the oxygen reduction reaction occurring on the cathode. In our current work the activation step was not carried out after supported catalyst synthesis. This deviation in procedure was necessitated by observation in tests trials that upon activation of the carbon mixture (25/75, 50/50 and 75/25) supported catalysts under nitrogen atmosphere at 350 °C, a drastic loss in weight occurred leading to the speculation that the activation step might be decomposing the Vulcan XC-72 carbon in the support mixture due to the possibility of air ingress into the reactor. The absence of an activation

procedure can potentially lead to larger agglomerates of platinum particles greater than 5 nm in size. However, the ramifications of this occurrence are potentially less severe than altering the composition of the support mixtures due to one of the components possibly burning off during activation step. Additionally the ethylene glycol route of colloidal platinum synthesis has been reported to reduce the platinum precursor directly to the metallic state [22]. This observation encouraged us to eliminate the activation step in our supported catalyst preparation in order to preserve the appropriate carbon support mixture ratio, while risking larger platinum particle sizes in the final supported catalyst system.

Platinum content (weight%) on the various carbon/carbon mixtures was determined by burning off the carbons under air atmosphere in a thermogravimetric analyzer (TGA; TGA-SDTA 851e, Mettler-Toledo Instruments) and recovering and weighing the residue. For comparison, a commercially available supported catalyst – 20% (by weight) platinum on Vulcan XC-72 carbon was obtained from E-TEK Inc., a division of BASF Fuel Cells. The commercially available supported catalyst was evaluated as a control supported catalyst sample for determination of platinum content and particle size. The Vulcan XC-72 carbon support in the commercial E-TEK catalyst had a reported BET surface area of 250 $m^2\,g^{-1}$ and an average platinum particle size of 2.2 nm [23].

Powder X-ray diffraction (XRD) patterns or diffractograms were recorded for the supported catalyst samples using a Scintag X-1 advanced X-ray diffraction system. The radiation employed was Cu-Kα (λ = 1.5418 Å). The angular region between 2θ values of 10° and 120° was scanned. A blank scan was run under similar conditions on a NIST Al_2O_3 standard to determine the instrumental broadening, which was subtracted while performing the particle size calculations.

2.2. Electrochemical analysis of supported catalyst

Hydrogen adsorption–desorption characteristics of the supported catalysts were determined by cyclic voltammetry (CV). Sample preparation was similar to the process outlined by Paulus et al. [24]. 10 mg of the supported catalyst sample was ultrasonically blended with 5 ml deionized water (Millipore SuperQ Systems; resistivity 18 MΩ cm), 5 ml of isopropanol and 40 μl of 5% liquid Nafion solution (Fluka). Thereafter, 20 μl of the homogenized solution was pipetted onto a 5 mm diameter glassy carbon rotating disk electrode (RDE) to uniformly cover an area of 0.196 cm^2 and allowed to dry in air. Calculations based on the platinum content (from the TGA data) on various carbons/mixtures yielded a platinum loading of 21–22 μg cm^{-2} on the glassy carbon disk. For each sample, the glassy carbon disk with the supported catalyst/Nafion film on it was immersed in a nitrogen de-aerated electrolyte (0.5 M H_2SO_4) and used as the working electrode (WE) in a three-electrode setup. A Luggin capillary with platinum gauze over which hydrogen was generated, served as the reversible hydrogen electrode (RHE) or the reference electrode (RE). A platinum wire in fritted glass tube was used as the counter electrode (CE). The working electrode potential was cycled several times between 0.045 V and 1.2 V (vs. the RHE) to initially remove any contamination and oxide formation on the working electrode surface. Room temperature hydrogen adsorption–desorption cyclic voltammogram were thereafter recorded between the potential limits of 0.4 V and 1.2 V (vs. RHE) at a scan rate of 20 mV s^{-1}.

2.3. MEA fabrication and evaluation of polarization behavior

Using the supported catalyst samples, electrode 'inks' were prepared via the well-known Los Alamos 'decal' method [4,5]. A representative ink mixture contained the supported catalyst, liquid Nafion binder (5 wt% in alcohol mixture, Fluka), glycerol (Aldrich) and 1 M tetrabutyl ammonium hydroxide in alcohol mixture (TBAOH, Fluka). The mixture was stirred in a glass vial until a homogeneous ink resulted. For the Pt/CNF and E-TEK samples, three ink compositions were prepared, wherein the weight ratio (w/w) between the supported catalyst and liquid Nafion binder was maintained at 5:2, 5:4 and 5:6, respectively. The ratios were varied to study the variation in fuel cell performance with increasing presence of Nafion in the catalyst ink and whether the trend was consistent for CNF and Vulcan XC-72 carbon (from the E-TEK catalyst).

Using a paint brush, thin layers of the ink were then painted onto one square side of double-sided PTFE-coated decals (area – 5 cm^2). Prior calculations dictated the weight of ink required to be painted on the decals to obtain a platinum loading of 0.3 mg cm^{-2} for both the anode and cathode. After each coating, the decals were dried in a vacuum oven at 210 °C for 20 min and weighed. The process of painting and drying in the oven was repeated until the desired ink weight was achieved. Platinum loadings for both the cathodes and anodes were kept equivalent.

Nafion® 115 membrane (average thickness 120 μm) obtained from Ion Power Inc., New Castle, DE was employed to fabricate MEAs. Prior to MEA preparation, 50 cm^2 square membrane pieces were first boiled in 5% H_2O_2 and thereafter 0.5 M H_2SO_4. Subsequently, the membrane pieces were ion-exchanged to Na^+ form overnight in a dilute solution of Na_2SO_4. The sodium form has superior thermal stability to withstand the hot press procedure employed in adhering electrodes to the membrane [4,25].

Each piece of membrane was subsequently sandwiched between two painted decals (cathode and anode) and hot-pressed in order to transfer the ink from decal to the membrane. Decal backings were then peeled off and the MEAs reconverted to their protic forms by boiling in 0.5 M sulfuric acid for 2 h and subsequently dried.

For polarization curve measurements, each MEA was assembled along with PTFE-coated fiberglass gaskets and 5 cm^2 gas diffusion layers (GDL) (ELAT® high pressure GDL) in a single cell test fixture with stainless steel end plates and graphite collector channels. The single cell was then connected to a fuel cell test station (FCT 2000, Fuel Cell Technologies Inc., Albuquerque, NM) coupled to a load box (Agilent Technologies, 6063 B, 250 W, 0–10 A, 3–240 V) and interfaced with a computer through a National Instruments Lab VIEW program. Temperatures of the anode (hydrogen) and cathode oxidant (air or oxygen) inlet streams and humidifiers were set at 85 °C. Gas flow rates at both cathode and anode lines were maintained at 100 sccm; the temperature of the cell hardware was held at 80 °C. A backpressure of 15 psi (1 atm.) was applied to both inlet fuel lines. The cell was maintained at open-circuit or no load conditions until the target temperature and pressure parameters were attained. Reproducible *V–I* characteristics of the MEA were subsequently measured in the form of galvanodynamic polarization curves with data points recorded at current intervals of 50 mA. The time period between each data point measurement was 30 s.

3. Results and discussion

3.1. Surface area of support mixtures and platinum content

Catalyst support mixtures had been prepared by mixing together lower surface area fibers (acid-functionalized carbon nanofibers) with lower surface area particulates (Vulcan XC-72). BET surface areas were determined for the baseline carbon supports and their mixtures prior to platinum deposition. Table 1 highlights the BET surface areas of the various carbon supports. The baseline acid-functionalized CNF had a BET surface of 127 $m^2\,g^{-1}$ while the Vulcan XC-72 had a BET surface area of 234 $m^2\,g^{-1}$. It would be

Table 1
BET surface area of various support/support mixtures and average platinum content determined from TGA curves.

Supported catalyst system	BET surface area of support ($m^2\ g^{-1}$)	Average platinum content (wt%)
Pt/Vulcan XC-72	234.9	22.3
Pt/(CNF/Vulcan-25/75)	184.8	20.6
Pt/(CNF/Vulcan-50/50)	147.6	20.5
Pt/(CNF/Vulcan-75/25)	80.5	20.4
Pt/CNF	127.1	18.8
Pt/Vulcan XC-72 [E-TEK commercial supported catalyst]	234.9	23.9

expected that the BET surface area values for the mixtures would follow their weighed averages. This is because the two types of supports (one amorphous and the other graphitic exist together in a mixture without any interaction with each other, therefore agglomeration does not occur). As is clear from Table 1, this belief is upheld by the BET surface area values for the CNF/Vulcan XC-72 – 25/75 and 50/50 mixtures. Comparison of their BET values indicates that the surface areas for the mixtures decrease with increasing CNF weight content. However, the BET area for the 75/25 mixture is abnormally low whereas the expectation was that it should be higher than the corresponding value for 100% CNF – 127 $m^2\ g^{-1}$. This result is possibly an outlier due to potential error and/or inaccuracy in measurement and in reality the BET surface area of the 75/25 mixture should lie in between the corresponding values for the baseline support and the 50/50 mixture – 147.6 $m^2\ g^{-1}$. Overall, the surface areas were not very high and therefore the various carbon mixtures, like their parent constituents, could also be classified as lower surface area carbon supports.

Platinum was subsequently deposited on the carbon support mixtures and the control supports by the glycol route and the platinum content estimated by gravimetric analysis. Representative TGA curves are indicated in Fig. 1 for the control carbon supports – 100% functionalized CNF and Vulcan XC-72, respectively. The average platinum loading (in weight% of platinum) is also illustrated in Table 1 for the various carbons and their mixtures. The concentration of preparatory iron catalyst on the CNF (which is less than 100 ppm) does not affect the calculated platinum content. In addition, the acid-modification procedure carried out on the CNF digests remnants of any remaining preparatory metal catalyst. From the TGA data in Table 1, the average platinum content on the carbon support mixtures is in close equivalence with that on the control carbon supports. The TGA results indicate that for lower surface area supports and their mixtures, the interaction of the platinum colloid with the mixed morphology carbon supports appears to be not qualitatively different from the interaction with either the functionalized carbon nanofibers or the Vulcan XC-72 carbon surfaces. The fact that the platinum content and particle sizes on the three support mixtures (CNF/Vulcan XC-72 – 25/75, 50/50 and 75/25) are similar to that obtained on the individual support is an indication that the chemical reactivity of the platinum colloids towards these supports is quite similar. Another reason for the equivalence in the platinum content is the boundary set by the BET surface areas for the mixed carbons, which for most part, lies between the values for the control supports (Table 1) with the exception of the outlier result for the (CNF/Vulcan XC-72/75/25) mixture. Thus, the mixture of supports offers no advantage in fostering the deposition of a higher weight percentage of platinum relative to the individual supports. This is perhaps not surprising, since the density of the nucleating sites for deposition of colloidal platinum is not augmented by simply mixing the carbons in a certain ratio. An additional conclusion from the platinum content data in Table 1 is that the ethylene glycol method applied for depositing platinum onto the lower surface area supports leads to platinum loadings that match the platinum content on the commercially available E-TEK sample.

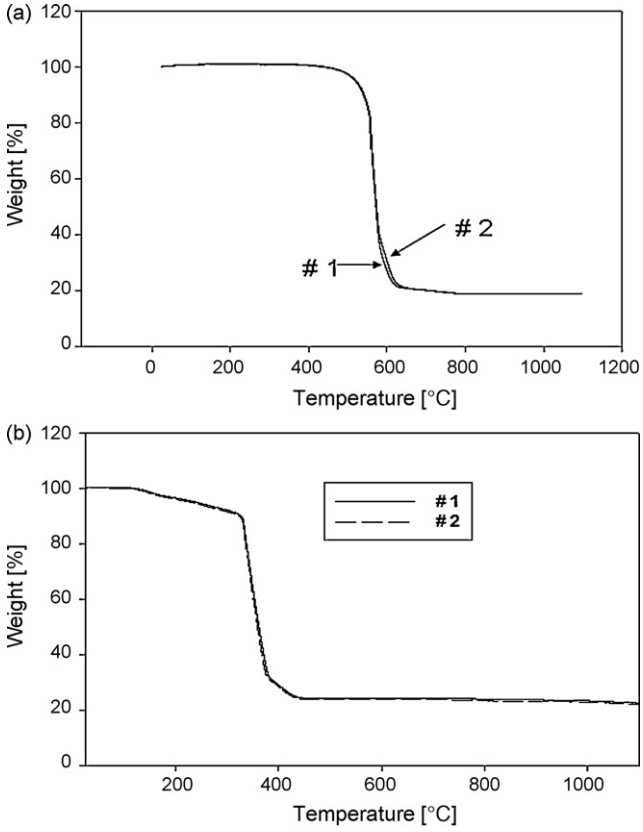

Fig. 1. TGA curves for platinum deposited on control carbon supports by the glycol method – 100% carbon nanofibers (a) and 100% Vulcan XC-72 carbon (b).

3.2. Platinum particle size on carbon supports

X-ray diffraction spectrums of platinum particles deposited on various carbons and their mixtures are indicated in Fig. 2(a–e). All of analyzed samples display the characteristic platinum peaks [1 1 1], [2 0 0], [2 2 0] and [3 1 1] corresponding to a face centered cubic (*fcc*) crystal lattice structure for the deposited platinum nanoparticles. The XRD patterns for samples with a greater fraction of CNF indicate a very sharp and symmetrical graphite peak – [0 0 2] which is a measure of the high overall crystallinity of the sample due to the ordered nature of graphite. On the other hand, the [0 0 2] peak for samples containing greater fraction of Vulcan XC-72 are very broad and lack intensity due to the amorphous nature of the Vulcan support. From the diffraction spectrums it is clear that the platinum [2 2 0] peak is positioned in isolation from the carbon support peaks and therefore can be used in the calculation of the mean platinum crystallite size. The platinum [2 2 0] reflection isolated from the XRD patterns of the various supported catalysts is also illustrated in the inset in Fig. 2(a–e). Fig. 3 indicates the corresponding XRD diffraction spectrum for the commercial E-TEK catalyst. A Gaussian curve was fitted to the [2 2 0] peak for each supported catalyst after correction for instrumental broadening. The correction gave a symmetrical [2 2 0] peak, from which the average platinum particle sizes were calculated using the Debye–Scherrer equation [26].

Table 2 compares the average platinum crystallite sizes (in nm) on the various carbons and their mixtures. There appears to be no trend in particle size with the nature of the support and its surface area (Table 1). Average particle sizes on the two control supports – 100% CNF and 100% Vulcan XC-72 carbon were similar to each

Table 2
Averaged platinum particle size determined from Gaussian curve fitting of Pt [2 2 0] peak for the various supported catalyst systems and commercially available E-TEK catalyst.

Supported catalyst system	Average platinum particle size (nm)
Pt/Vulcan XC-72	3.7
Pt/(CNF/Vulcan-25/75)	4.6
Pt/(CNF/Vulcan-50/50)	4.3
Pt/(CNF/Vulcan-75/25)	3.4
Pt/CNF	3.7
Pt/Vulcan XC-72 [E-TEK commercial supported catalyst]	2.4

other. One fact that should be kept in mind is that the supported catalyst samples had not been heat-treated (as discussed earlier), as is typical done after catalyst preparation by the glycol route. Lack of an activation step may have caused the particle sizes to be larger than expected because prior to the activation stage, the platinum colloidal particles are vulnerable to aggregation. Nevertheless, the sizes determined were fairly close to each other and most importantly, they all lied in the 2–5 nm size range, which is the size range desired for optimum catalytic activity [22]. The similarity in particle sizes supported the belief that the platinum deposition on the lower surface area carbons was not influenced in any significant manner by the support morphology and surface area.

3.3. Influence of Nafion content on polarization behavior

Fuel cell polarization performances were evaluated for CNF and E-TEK MEAs fabricated with decreasing ratios of supported catalyst to Nafion in the electrode ink mixture – 5:2, 5:4 and 5:6, respectively. The ratios were altered to study the variation in fuel cell performance with increasing presence of Nafion in the catalyst ink. The fuel cell performance for the mixed carbon supported catalyst systems were not compared to the lack of a quantity sufficient enough to fabricate MEAs with varying contents of the Nafion

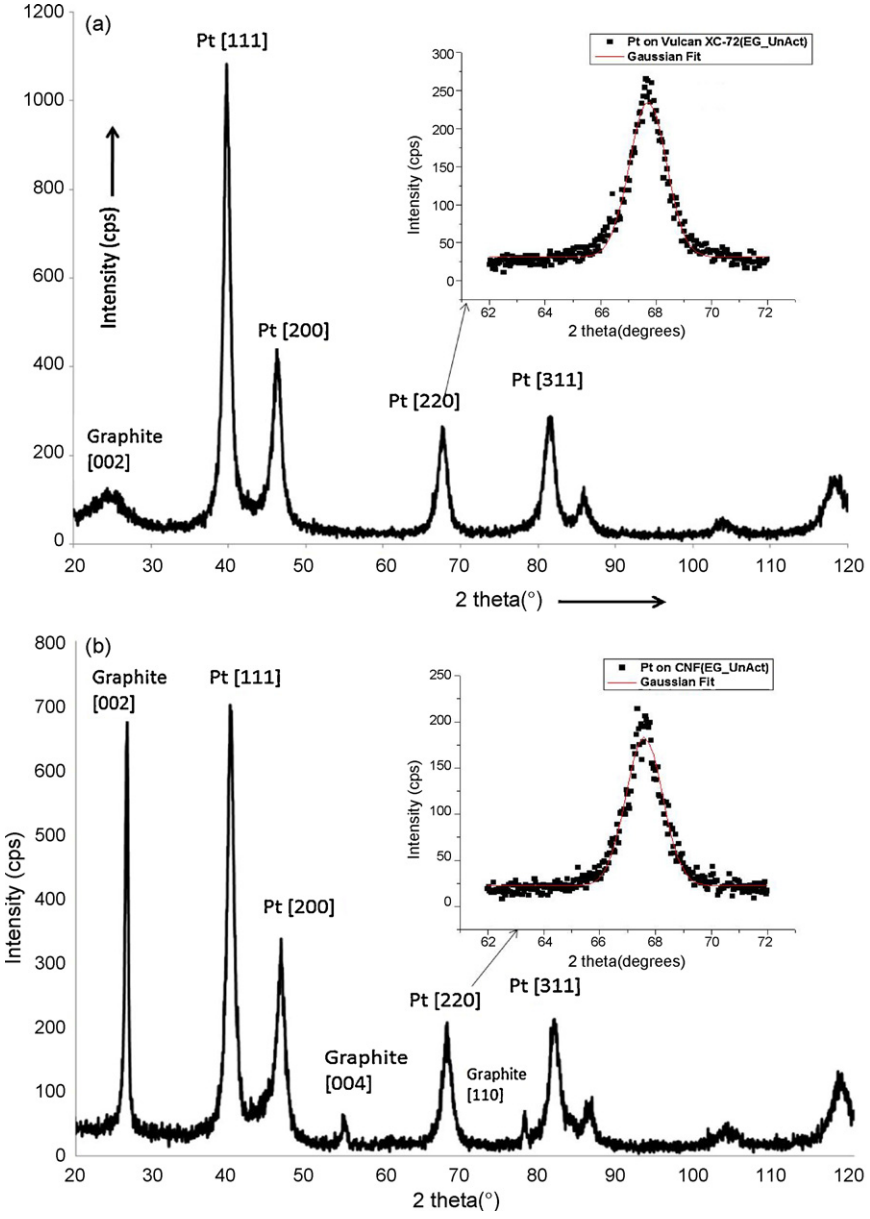

Fig. 2. X-ray diffraction (XRD) spectrums for platinum deposited on various carbon supports and their mixtures. Image in inset indicates the Gaussian curve fitted Pt [2 2 0] peak from the XRD diffraction spectrum (a) control support – 100% (by weight) Vulcan XC-72, (b) control support – 100% (by weight) CNF, (c) (CNF/Vulcan-25/75) support mixture, (d) (CNF/Vulcan-50/50) support mixture and (e) (CNF/Vulcan-75/25) support mixture.

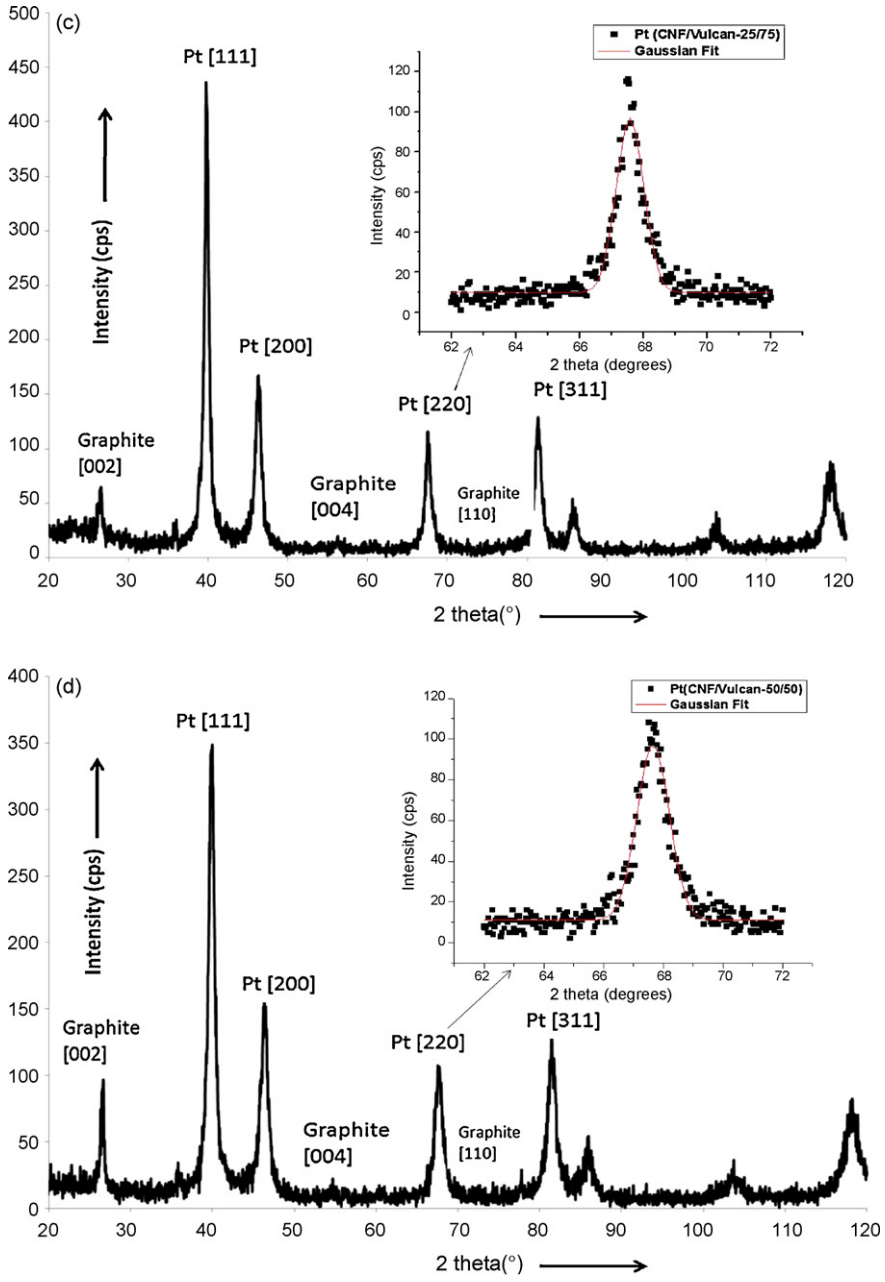

Fig. 2. (*Continued*).

binder. Since 100% CNF and 100% Vulcan XC-72 (within the E-TEK MEA), represented the two extremes for the types of carbon supports investigated in this work, it was considered appropriate to considered appropriate enough to compare and contrast only those two on a one-on-one basis. SEM images in Fig. 4 compare the surface of a Teflon decal coated with Pt/CNF ink to the surface of another Teflon decal coated with the E-TEK catalyst ink. Calculated platinum loading is 0.3 mg cm^{-2}. Supported catalyst to liquid Nafion ratio for the images depicted is 5:2. Clearly, the CNF MEA appears has a 'mat-like' appearance due to the presence of the cylindrical nanofibers while the E-TEK MEA has a smoother surface.

Fig. 5 compares the MEA polarization curves for (a) CNF and (b) E-TEK MEAs prepared using varying ratios of supported catalyst to Nafion in catalyst ink (5:2, 5:4 and 5:6). The trends in performance for MEAs with decreasing carbon loadings in the electrode ink appear identical for the CNF and E-TEK catalyst systems. Polarization curves for MEAs with half the normal loading of carbon (i.e. fabricated from the ink consisting of 5:4 supported catalyst:Nafion binder) nearly overlapped the curves with the conventional loading (which as per the decal-method was set to 5:2). The major drop in polarization performance appears to lie somewhere between the one-half (5:4) and one-third (5:6) carbon loadings. From the polarization curves in Fig. 5, for 5:2 ratio, the E-TEK MEA gives a performance of about 0.6–0.65 A cm^{-2} @ 0.65 V. The corresponding value for the Pt/CNF MEA is about 0.45–0.5 A cm^{-2} @ 0.65 V. It is possible that the lack of an activation stage led to the larger platinum particles (on the CNF support) and hence a lower performance than the commercial E-TEK sample. We have indicated in our published results that the electrochemically active surface area of platinum deposited on functionalized CNF (the supported catalyst sample being activated in that case) is very close to that of the 20% E-TEK sample [15]. Additionally, from rotating disk electrode studies, the corresponding Tafel slopes towards ORR are also very close to each other [15]. For both the CNF and E-TEK MEAs,

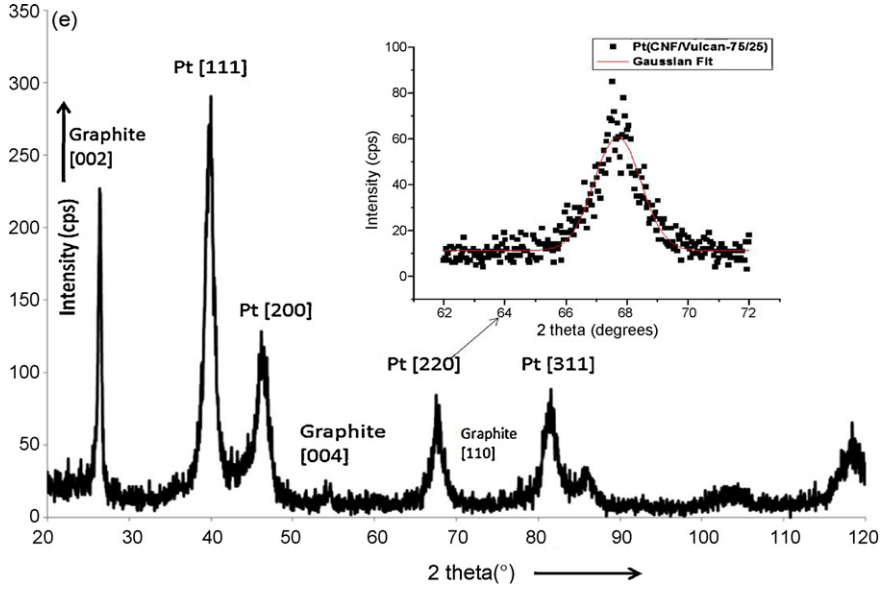

Fig. 2. (*Continued*).

there is a sharp drop in the polarization behavior beyond open-circuit voltage for the one-third carbon loading. This result is likely due to a poorly connected three-dimensional electronic conduction network in the MEA at the very low carbon loadings. Also, the high loading of Nafion binder in the catalyst ink, inhibits gas access to the platinum catalyst particles. This result, for both types of carbon supports is consistent with the literature observation that increasing the liquid ionomer loading beyond a certain threshold lowers the platinum sites available for catalysis and retards oxygen transport within the MEA [27,28].

One might expect the fibrous/cylindrical CNF, with its superior electronic conductivity, to display a constant polarization behavior even at low carbon loadings (such as the 5:6 ratio). However, as can be clearly seen in Fig. 5(a), the CNF MEA with one-third the typical carbon loading also exhibits poor fuel cell performance. The major conclusion that one can derive is that for the catalyst loading used in this work, the two lower surface area supports – CNF and Vulcan XC-72 (from the E-TEK catalyst) display fairly similar electrochemical performance trends even if the amount of carbon is reduced (relative to the Nafion binder in the MEA). There exists a threshold of supported catalyst loading which will lead to a drastic drop in fuel cell performance. For the supported catalysts and electrodes investigated in our work, this threshold lies somewhat between a weight ratio of 5:4 (supported catalyst to Nafion) and 5:6. The observation of similar performance for the 5:4 ratio to that of the 5:2 ratio (for both types of samples tested) indicates that the addition of fibrous material alters somewhat the network connectivity in the catalyst layer such that substantially lower amounts of carbon to platinum provide satisfactory connectivity. This additional degree of freedom may be helpful in designing improved catalyst layers. However, it is important to note that these observations are tied to a specific method of electrode fabrication.

3.4. Hydrogen adsorption desorption cyclic voltammetry

Room temperature HAD cyclic voltammograms for the various supported catalysts were recorded in 0.5 M de-aerated sulfuric acid electrolyte. Fig. 6 indicates the CVs for the supported catalysts. From the CVs, the double layer capacitance (0.4–0.6 V vs. RHE) appeared to be larger for the Pt/Vulcan XC-72 (100%) supported catalyst system and the Pt/(25/75) CNF/Vulcan XC-72 catalyst systems. This is as expected since these carbons have the two largest BET surface areas amongst the carbons utilized in our work (Table 1). Hydrogen adsorption–desorption peaks were visible for all the supported

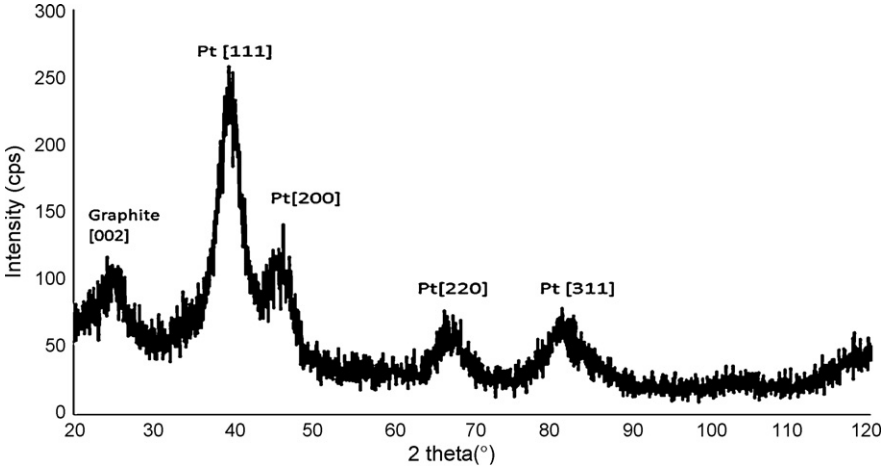

Fig. 3. X-ray diffraction (XRD) spectrum for commercially available E-TEK catalyst – 20% (by weight) Pt on Vulcan XC-72 carbon.

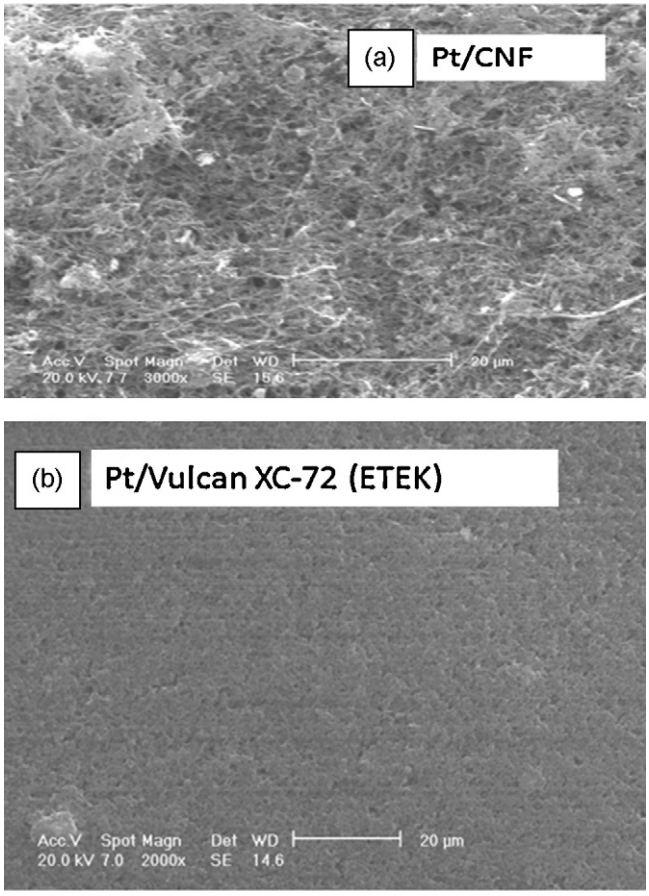

Fig. 4. SEM image depicting the morphological characteristics of supported catalyst ink painted onto a Teflon decal for MEA fabrication – (top) Pt/CNF catalyst ink and (bottom) commercially available E-TEK catalyst (20% Pt on Vulcan XC-72 carbon).

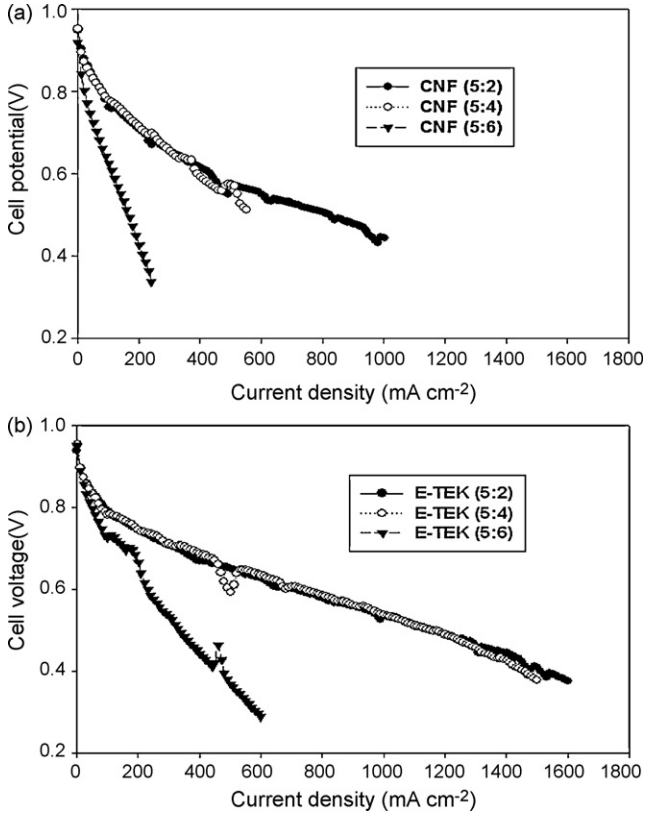

Fig. 5. Cell polarization curves for (a) CNF and (b) E-TEK MEAs prepared using varying ratios of supported catalyst to Nafion in catalyst ink (5:2, 5:4 and 5:6). Anode fuel – hydrogen, cathode oxidant – oxygen. Platinum catalyst loadings on anode and cathode are 0.3 mg cm^{-2}. Membrane-Nafion 115. Operating conditions are T_{cell} = 80 °C, $T_{Humidifier\ (cathode\ and\ anode)}$ = 85 °C, backpressure (cathode and anode) = 15 psig.

catalyst systems with no noticeable shift in the platinum oxide peak potentials. From a first order estimate, the nearly overlapping desorption region of the CVs indicated that the electrochemically active surface area (ESA) of platinum on the various carbons would be nearly equivalent. This result is not surprising as the platinum content and the particle sizes on the various carbon mixtures (and the control supports) were very close to each other. From an electrochemical point of view, this observation would translate to potentially identical available surface areas of the supported catalyst samples for the fuel cell reactions (especially ORR). This result also points towards the primary conclusion of this work, which is that for the lower surface area supports investigated in this work, support morphology has a negligible influence on the electrochemical response of the catalyst deposited on its surface. Certainly an in-depth probing into the kinetic parameters of the platinum on the mixed carbons, such as the determination of Tafel slopes and exchange current densities would be a logical next step towards definitively comparing and contrasting these catalyst systems for extensive use in fabricating PEM fuel cell MEAs. As mentioned in the previous section, our previous published work has carried out RDE studies to compare the electrochemical activity of Pt/CNF with E-TEK catalysts towards ORR and found that they are very comparable [15]. Also their electrochemically active surface areas (EAS) from hydrogen adsorption–desorption cyclic voltammograms (CV) were found to be comparable as well. One of the objectives of this work was to also probe if the platinum particle size and platinum content varied when a mixture of low-surface area carbon supports was employed. Judging by the equivalence in the platinum particles sizes, platinum content and the CV shape (from Fig. 6), the electrochemical activity of the Pt on the mixed carbon supports should be the same as the baseline supports – CNF and Vulcan XC-72. Certainly extensive electrochemical testing is required to further this belief, which is beyond the scope of the current discussion.

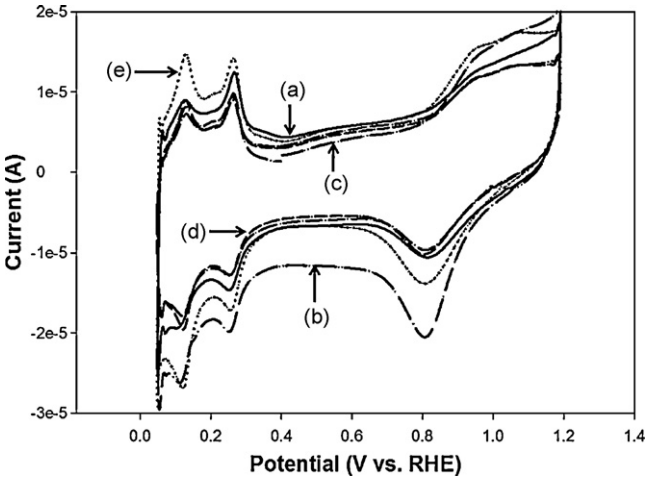

Fig. 6. Room temperature hydrogen adsorption/desorption cyclic voltammogram for platinum deposited on various carbons and their mixtures. Electrolyte is de-aerated 0.5 M H_2SO_4 and scan rate is 20 mV s^{-1}. (a) Control support – 100% (by weight) Vulcan XC-72, (b) (CNF/Vulcan-25/75) support mixture, (c) (CNF/Vulcan-50/50) support mixture, (d) (CNF/Vulcan-75/25) support mixture and (e) control support – 100% (by weight) CNF.

4. Conclusions

Lower surface area supports, especially carbon nanofibers and Vulcan XC-72 carbon can aid in fuel cell performance by enhancing the electronic conductivity in a PEM fuel cell and are often preferred over higher surface area supports. For the range of supported catalyst loadings that have been employed in the inks used to fabricate the MEAs, the unique morphology of either lower surface area carbon – CNF and Vulcan XC-72, has no bearing on the corresponding polarization behavior of the MEA. Additionally, for both the control carbon supports, the fuel cell polarization behavior has a threshold point based on the amount of carbon present in the supported catalyst used to fabricate the MEA. Interestingly, this threshold point is different from that observed for similarly prepared XC-72-based catalyst layers.

Acknowledgements

The authors acknowledge the support provided by the U.S. Army Research Office for this work through the MURI program contract number DAAD 190310169.

Pyrograf® is a registered trademark of Applied Sciences Inc., Cedarville, OH; Norit® is a registered trademark of Norit Americas Inc., Marshall, TX; Vulcan® is a registered trademark of Cabot Corporation, Billerica, MA; E-TEK^{sm} is a registered service mark of BASF Fuel Cell Inc. E-TEK Division, Somerset, NJ; E-LAT® is a registered trademark of BASF Fuel Cell Inc. E-TEK Division, Somerset, NJ; Teflon® and Nafion® are registered trademarks of E.I. DuPont de Nemours and Company, Wilmington, DE.

References

[1] L. Giorgi, E. Antolini, A. Pozio, E. Passalacqua, Electrochim. Acta 43 (1998) 3675.
[2] S.J. Lee, S. Mukerjee, J. McBreen, Y.W. Rho, Y.T. Kho, T.H. Lee, Electrochim. Acta 43 (1998) 3693.
[3] J. Xie, F. Garzon, T.A. Zawodzinski, W. Smith, J. Electrochem. Soc. 151 (2004) A1084–A1093.
[4] M.S. Wilson, S. Gottesfeld, J. Appl. Electrochem. 22 (1992) 1–7.
[5] M.S. Wilson, US Patent 5,211,984 (1993).
[6] A.P. Saab, F.H. Garzon, T.A. Zawodzinski, J. Electrochem. Soc. 149 (2002) A1541.
[7] V. Stanic, Electrochem. Soc. Proc. 31 (2002) 315.
[8] Z. Wang, Y. Liu, V.M. Linkov, J. Power Sources 160 (2006) 326.
[9] X. Yu, S. Ye, J. Power Sources 172 (2007) 133–144.
[10] J. Kaiser, P.A. Simonov, V.I. Zaikovskii, C. Hartnig, L. Jorissen, E.R. Savinova, J. Appl. Electrochem. 37 (2007) 1429–1437.
[11] E. Antolini, R.R. Passos, E.A. Ticianelli, J. Power Sources 109 (2002) 477–482.
[12] W.H. Lizcano-Valbuena, V.A. Paganin, C.A.P. Leite, F. Galembeck, E.R. Gonzalez, Electrochim. Acta 48 (2003) 3868–3878.
[13] J. Marie, S. Berthon-Fabry, M. Chatenet, E. Chainet, N. Pirard, N. Cornet, P. Achard, J. Appl. Electrochem. 37 (2007) 147–153.
[14] L. Calvillo, M. Gangeri, S. Perathoner, G. Centi, R. Moliner, M.J. Lazaro, J. Power Sources 192 (2009) 144–150.
[15] A. Guha, T.A. Zawodzinski, D.A. Schiraldi, J. Power Sources 172 (2007) 530–541.
[16] W. Yu, W. Tu, H. Liu, Langmuir 15 (1999) 6–9.
[17] W. Tu, H. Liu, Chem. Mater. 12 (2000) 564–567.
[18] Z. Liu, J.Y. Lee, W. Chen, M. Han, L.M. Gan, Langmuir 20 (2004) 181–187.
[19] http://www.apsci.com/ppi-pyro3.html.
[20] A. Guha, T.A. Zawodzinski, D.A. Schiraldi, Carbon 45 (2007) 1506–1517.
[21] C.W.B. Bezerra, L. Zhang, H. Liu, K. Lee, A.L.B. Marques, E.P. Marques, H. Wang, J. Zhang, J. Power Sources 173 (2007) 891–908.
[22] W. Li, C. Liang, W. Zhou, J. Qiu, H. Li, G. Sun, Q. Xin, Carbon 42 (2004) 436–439.
[23] http://www.etek-inc.com/pdfs/Catalyst_ProductCatalog.pdf.
[24] U.A. Paulus, T.J. Schmidt, H.A. Gasteiger, R.J. Behm, J. Electroanal. Chem. 495 (2001) 131–145.
[25] S.H. de Almeida, Y. Kawano, J. Therm. Anal. Calorim. 58 (1999) 569–577.
[26] V. Radmilović, H.A. Gasteiger, P. Ross Jr., J. Catal. 154 (1995) 98–106.
[27] Naryanamoorthy, S. Durairaj, Y. Song, Y. Xu, J. Choi, J. Appl. Phys. Lett. 90 (2007) 063112.
[28] J.M. Song, S.Y. Cha, W.M. Lee, J. Power Sources 94 (2001) 78–84.